



ELSEVIER

Contents lists available at ScienceDirect

## Journal of Materials Science &amp; Technology

journal homepage: [www.elsevier.com/locate/jmst](http://www.elsevier.com/locate/jmst)

## Research Article

## Unexpected non-monotonic changing in the heterogeneity of glasses during annealing

Yu Tong<sup>a</sup>, Fucheng Li<sup>b</sup>, Lijian Song<sup>a</sup>, Yanhui Liu<sup>b</sup>, Juntao Huo<sup>a</sup>, Jichao Qiao<sup>c,\*</sup>, Yao Yao<sup>c</sup>, J.M. Pelletier<sup>d</sup>, Daniel Crespo<sup>e</sup>, Eloi Pineda<sup>e,\*</sup>, Jun-Qiang Wang<sup>a,\*</sup><sup>a</sup> CAS Key Laboratory of Magnetic Materials and Devices, and Zhejiang Province Key Laboratory of Magnetic Materials and Application Technology, Ningbo Institute of Materials Technology and Engineering, Chinese Academy of Sciences, Ningbo 315201, China<sup>b</sup> Institute of Physics, Chinese Academy of Sciences, Beijing 100190, China<sup>c</sup> School of Mechanics, Civil Engineering and Architecture, Northwestern Polytechnical University, Xi'an 710072, China<sup>d</sup> Mateis, UMR CNRS5510, INSA-Lyon, Université de Lyon, Villeurbanne cedex F-69621, France<sup>e</sup> Department of Physics, Institute of Energy Technologies, Universitat Politècnica de Catalunya, Barcelona 08019, Spain

## ARTICLE INFO

## Article history:

Received 26 May 2023

Revised 19 July 2023

Accepted 27 July 2023

Available online 20 September 2023

## Keywords:

Glasses

Heterogeneity

Aging

Relaxation

## ABSTRACT

The heterogeneity of glasses has critical influences on the properties. How heterogeneity evolves during annealing is an intriguing cutting-edge question. In this work, the heterogeneity of the annealed metallic and polymer glasses has been studied systematically by using stress relaxation and nanoindentation tests. The stress relaxation processes are analyzed using Kohlrausch-Williams-Watts (KWW) equation. We surprisingly find that the heterogeneous factor  $\beta_{KWW}$  in KWW equation does not change monotonously but increases first and then decreases along with the annealing time. The two-stage process implies that glasses do not evolve as expected toward the more homogeneous glassy state but become homogeneous first and then more heterogeneous. This is further verified by the evolution of critical shear stress for local plasticity. It is revealed that the two-stage process is correlated with different relaxation modes, which is further interpreted using a phenomenological model. These findings not only give insights into understanding the nature of glasses, but also are useful for designing glasses with superior properties.

© 2023 Published by Elsevier Ltd on behalf of The editorial office of Journal of Materials Science & Technology.

## 1. Introduction

Glasses are a family of disordered materials which are macroscopically homogeneous but microscopically heterogeneous [1–7]. The heterogeneous microstructures have critical influences on the properties of glasses. For example, the nanoscale liquid-like flow units correlate with the fast relaxation kinetics and determine the plasticity of metallic glasses [7–16], and the nanoscale structural fluctuations couple with the magnetic domain walls and influence the soft magnetism of metallic glasses [17–19]. Thus, it attracts intense interest to study the evolution of nanoscale heterogeneity, especially during annealing [2,20–23]. Upon annealing, glasses usually evolve toward the equilibrium configuration [22,24]. It is expected that isothermal aging promotes the homogeneity of glasses due to the annihilation of mobile domains and the release of residual stress [5,25,26]. However, some experimental and simulation results show the opposite results [27,28]. Furthermore, it has been

demonstrated that the isothermal aging process in glasses involves multiple distinct stages [16,29–38], as evidenced by various physical variables such as the change of activation energy [32,39] and density [29,35]. However, how the heterogeneity changes during these stages remains unclear. Unraveling the aging effects on heterogeneity is beneficial not only for designing advanced metallic glasses but also for understanding the nature of glasses.

The heterogeneity of glasses can be explored through stress relaxation tests [29,33,38,40,41]. Owing to the multiple relaxation processes with different time scales and structural cooperative rearrangements [8,29,38,42]. The relaxation process usually exhibits non-exponential characteristics, which can be well-fitted using the non-exponential Kohlrausch-Williams-Watts (KWW) equation. The stretching exponent  $\beta_{KWW}$  in the KWW equation is an ideal parameter to reflect the heterogeneity of glasses. A smaller  $\beta_{KWW}$  denotes stronger heterogeneity, broader relaxation time spectrum, and more dispersed energy spectra [28,43]. The kinetic heterogeneity in structural rearrangement processes is far more drastic than the changes observed in volume, enthalpy, or other 'static' properties [28,29,44]. This makes stress relaxation an intriguing strategy to detect the effects of aging on glass heterogeneity.

\* Corresponding authors.

E-mail addresses: [gjczy@nwpu.edu.cn](mailto:gjczy@nwpu.edu.cn) (J. Qiao), [eloi.pineda@upc.edu](mailto:eloi.pineda@upc.edu) (E. Pineda), [jqwang@nimte.ac.cn](mailto:jqwang@nimte.ac.cn) (J.-Q. Wang).

In this letter, we have studied the effects of aging on the dynamical and structural heterogeneities of the three representative metallic glasses (MGs) and a polymer glass (Polyvinyl chloride, PVC) by following the stress relaxation and nanoindentation tests, respectively. An unexpected two-stage aging behavior is manifested by a clear turning point of the stretching exponent  $\beta_{\text{KWW}}$ . Our finding suggests that the effect of aging on the heterogeneity of the glassy dynamics is nonmonotonic, which is linked strongly to the nanoscale structural heterogeneity confirmed by the statistical fluctuation of critical shear stress for local plasticity. We also propose a phenomenological model and a microscopic structural picture to connect the relaxation dynamics observations with the evolution of structural heterogeneity during aging.

## 2. Materials and experiments

### 2.1. Sample preparation

The experiments are carried out in three representative metallic glasses with distinct physical properties, e.g.,  $\text{Ti}_{16.7}\text{Zr}_{16.7}\text{Hf}_{16.7}\text{Cu}_{16.7}\text{Ni}_{16.7}\text{Be}_{16.7}$  (at.%),  $\text{La}_{60}\text{Ni}_{25}\text{Al}_{15}$  (at.%), and  $\text{Fe}_{76}\text{Si}_9\text{B}_{10}\text{P}_5$  (at.%). The master ingots were fabricated by arc-melting under the ultra-high purity Ar atmosphere. Ribbon samples were obtained by melt-spinning, and the corresponding sample sizes (thickness  $\times$  width: mm) are  $0.043 \times 0.549$ ,  $0.03 \times 2.517$  and  $0.035 \times 1.360$  for Ti-, La-, and Fe-MG, respectively. Polyvinyl chloride films (size: 0.15 mm  $\times$  6.4 mm) are purchased from the manufactory.

### 2.2. Structural and dynamic characterization

Differential scanning calorimetry (DSC) was used to determine the glass transition temperature  $T_g$  with a heating rate of 20 K  $\text{min}^{-1}$ , as shown in Fig. S1(a,b) in Supplementary Information. The dynamic mechanical behavior was measured employing the dynamic thermomechanical analysis apparatus (TA DMA-Q800), as displayed in Fig. S1(c-f). The structure of the samples was characterized in a Talos F200X transmission electron microscope (TEM). According to the homogeneous maze-like pattern in high-resolution transmission electron microscopy (HRTEM) images and the diffraction halos, both the as-cast and annealed samples of TiZrHfCuNiBe MG were verified to be fully amorphous structures, as shown in Fig. S2.

### 2.3. Stress relaxation measurements

The isothermal stress relaxation tests after different aging times at various temperatures were performed on TA DMA-Q800. During the stress relaxation, the step strains applied on TiZrHfCuNiBe,  $\text{La}_{60}\text{Ni}_{15}\text{Al}_{25}$ ,  $\text{Fe}_{76}\text{Si}_9\text{B}_{10}\text{P}_5$  MGs and PVC are 0.1%, 0.3%, 0.3% and 0.5%, respectively. The time span of the stress relaxation tests for the TiZrHfCuNiBe,  $\text{La}_{60}\text{Ni}_{15}\text{Al}_{25}$ ,  $\text{Fe}_{76}\text{Si}_9\text{B}_{10}\text{P}_5$  MGs, and PVC are 9000 s, 3600 s, 3600 s, and 1800 s, respectively.

### 2.4. Nanoindentation tests

To evaluate spatial heterogeneity, nanoindentation tests were performed at room temperature using a TriboIndenter system (Bruker Hysitron TI980). The Berkovich tip was selected with an effective radius of  $R_{\text{tip}} = 360$  nm. The nanoindentation array contains 200 ( $20 \times 10$ ) indents, and the corresponding indent spacing is 5  $\mu\text{m}$ . The average surface roughness of untested TiZrHfCuNiBe films is about 1 nm (see Fig. S3(a)), which is much smaller than the indentation depth (Fig. S3(c)). Loading protocol: loading to a maximum force of 3000  $\mu\text{N}$  at a constant loading rate of 600  $\mu\text{N}$

$\text{s}^{-1}$ , followed by a holding segment of 2 s duration, and finally unloading to the zero within 5 s, as illustrated in Fig. S3(b). During the initial elastic stage, the smooth load-displacement ( $P$ - $h$ ) curves can be fitted by the Hertzian contact theory:  $P = \frac{4}{3}E_r\sqrt{R_{\text{tip}}}\cdot h^{\frac{3}{2}}$  [45,46], where  $E_r$  represents the reduced elastic modulus (Fig. S3(c)).

## 3. Results

### 3.1. Aging effect on dynamic heterogeneity

Fig. 1(a) illustrates the experiment protocol, which contains the isothermal annealing during different aging times  $t_a$  and the stress relaxation tests. The temperature of the whole experiment keeps at a constant temperature  $T_a$ , which is below the glass transition temperatures  $T_g$  (680 K for the  $\text{Ti}_{16.7}\text{Zr}_{16.7}\text{Hf}_{16.7}\text{Cu}_{16.7}\text{Ni}_{16.7}\text{Be}_{16.7}$  high-entropy MG, see Fig. S1), indicating high atomic mobility and out-of-equilibrium state. Fig. 1(b) shows the isothermal, tensile stress relaxation tests of TiZrHfCuNiBe MG after various  $t_a$  at the temperature of 633 K. The relaxation process can be well described by the Kohlrausch-Williams-Watts (KWW) function [8,47]:

$$\phi(t') = \frac{\sigma(t')}{\sigma_0} = \exp\left[-\left(\frac{t'}{\tau_{\text{KWW}}}\right)^{\beta_{\text{KWW}}}\right], \text{ with } t' = t - t_a \quad (1)$$

where  $\sigma$  and  $\sigma_0$  are the stress and initial stress, respectively.  $t$  is the time since the sample reaches temperature  $T_a$  and  $t'$  the time elapsed since the start of the relaxation test at  $t_a$ .  $\tau_{\text{KWW}}$  is the structural relaxation time. The stretching exponent  $\beta_{\text{KWW}}$  is associated with the dynamic heterogeneity of the system [8], larger  $\beta_{\text{KWW}}$  normally denoting the narrower relaxation time distribution and more homogeneous glassy system [3,5,8,40,48,49].

Fig. 1(c-f) shows the  $t_a$ -dependent parameters ( $\beta_{\text{KWW}}$ ,  $\tau_{\text{KWW}}$ ) for TiZrHfCuNiBe,  $\text{La}_{60}\text{Ni}_{25}\text{Al}_{15}$ ,  $\text{Fe}_{76}\text{Si}_9\text{B}_{10}\text{P}_5$  MGs and PVC polymer glass. Interestingly, the heterogeneous parameter  $\beta_{\text{KWW}}$  shows an unexpected non-monotonic behavior for all glasses, see Fig. 1(c) and (e). It increases for the short aging time (termed here as initial aging) and then decreases for the long aging time (termed as the deep aging regime). The structural relaxation time  $\tau_{\text{KWW}}$  (see Fig. 1(d, f)) shows an increasing trend with aging time. The evolution of  $\tau_{\text{KWW}}$  with  $t_a$  in two stages can be described by  $\tau_{\text{KWW}} = At_a^\mu$ , where  $\mu$  is the aging shift rate (or aging exponent), which signifies a rate of increase in the relaxation time concerning aging time and  $A$  is a parameter [50]. The same evolution trends of parameters ( $\beta_{\text{KWW}}$ ,  $\tau_{\text{KWW}}$ ) were obtained by two applied strains (0.1% and 0.5%) in TiZrHfCuNiBe MG (see Fig. S4), implying that the small-strain stress relaxation is effective for detecting the dynamic heterogeneity of pre-aging. It is worth noting that the three representative metallic glasses and the PVC polymer glass have distinct compositions that cover a wide range of physical properties, e.g., glass transition temperature, fragility, yield strength, and relaxation kinetics. This suggests that such a non-monotonous effect upon annealing is probably a universal characteristic for metallic glasses, or even for glasses, which challenges the current view of aging producing a continuous, monotonic change of the heterogeneity in disordered materials [27,38,43,50–52].

### 3.2. Aging effect on spatial heterogeneity

The microstructural heterogeneity of glass can be reflected sensitively by the critical shear stress  $\tau_c$  for the local plasticity because the loose packing domains exhibit lower  $\tau_c$  than dense packing domains [11,12,27,46,53,54]. In nanoindentation load-displacement ( $P$ - $h$ ) curves,  $\tau_c$  can be determined using the equation  $\tau_c = 0.31\left(\frac{6E_r^2}{\pi^3 R_{\text{tip}}^2} \cdot P_{\text{pop-in}}\right)^{\frac{1}{3}}$ , where  $P_{\text{pop-in}}$  corresponds to the loading

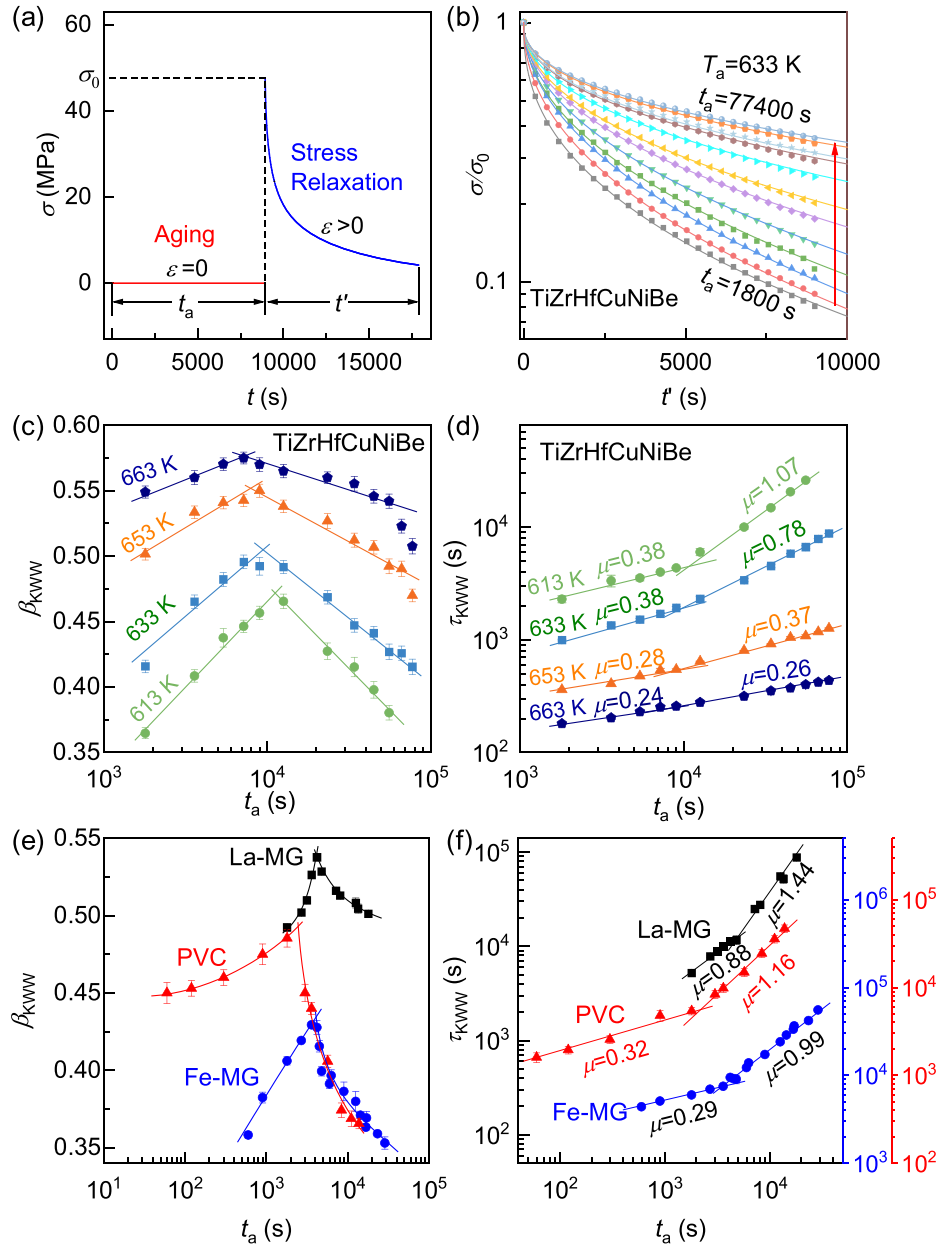


**Fig. 1.** Pre-aging effects on dynamical heterogeneity. (a) Schematic description of the experiment protocol, which includes the isothermal aging stage without stress and the stress relaxation stage at a fixed strain  $\varepsilon$ . (b) Stress (normalized to initial stress,  $\sigma/\sigma_0$ ) relaxations of TiZrHfCuNiBe MGs after being aged at  $T_a = 633$  K for  $t_a = 1800$ –77,400 s. The data can be well-fitted using the KWW equation (solid curves). (c–f) Two-stage evolution of dynamical heterogeneity for three representative metallic glasses and a polymer glass, e.g., TiZrHfCuNiBe,  $\text{La}_{60}\text{Ni}_{25}\text{Al}_{15}$ ,  $\text{Fe}_{76}\text{Si}_9\text{B}_{10}\text{P}_5$ , and PVC: (c) and (e) Heterogeneous factor  $\beta_{\text{KWW}}$  first increases but then decreases after long-time annealing; (d) and (f) Aging time dependent  $\tau_{\text{KWW}} = At_a^\mu$  at different temperatures. The slope  $\mu$  is larger in the second stage compared to the first stage. The experimental temperatures  $T_a$  for  $\text{La}_{60}\text{Ni}_{25}\text{Al}_{15}$ ,  $\text{Fe}_{76}\text{Si}_9\text{B}_{10}\text{P}_5$ , and PVC are 360, 643, and 328 K, respectively.

forces at the first pop-in event indicating the onset of plasticity [45,55] (see Fig. 2(a)). Fig. 2(b) shows statistical distributions of the  $\tau_c$  ( $\tau_c$ -distribution) for TiZrHfCuNiBe samples after pre-annealing at 633 K with various  $t_a$ . The wide distribution of  $\tau_c$  confirms the microstructural heterogeneity [46,53,56,57]. During the initial aging stage ( $t_a \leq 9000$  s, before the turning point of the  $\beta_{\text{KWW}}$ ), the mean value of  $\tau_c$  increases fast, while the distribution width (indicated as the full width at half maximum, FWHM) becomes narrower, as shown in Fig. 2(c, d). The narrower distribution suggests a more homogeneous structure, which is consistent with the increase of  $\beta_{\text{KWW}}$ . The accompanying increase in  $\tau_c$  indicates that the atomic packing becomes denser in mobile domains, which results in a more homogeneous structure. In the deep aging state ( $t_a > 9000$  s), the  $(\tau_c)_{\text{mean}}$  does not change much, but the  $\tau_c$ -

distribution broadens a lot, which suggests the increase of structural heterogeneity, which is consistent with the aforementioned declining  $\beta_{\text{KWW}}$ .

#### 4. Discussion

To unravel the underlying physical origin, we studied the thermal activation kinetics during aging. The activation energy  $E_a$  during structural relaxation is calculated by using the Arrhenius equation:  $\tau_{\text{KWW}} = \tau_E \exp(\frac{E_a}{RT})$ , where  $\tau_E$  and  $R$  represent the pre-exponential factor and gas constant, respectively [5]. Fig. 3(a) shows the  $t_a$ -dependent  $E_a$  of TiZrHfCuNiBe. For the initial aging stage, the  $E_a$  is around  $27.0(\pm 0.2)RT_g \approx 152.2$  kJ/mol, which is almost equal to the empirical activation energy of the  $\beta$  relaxation

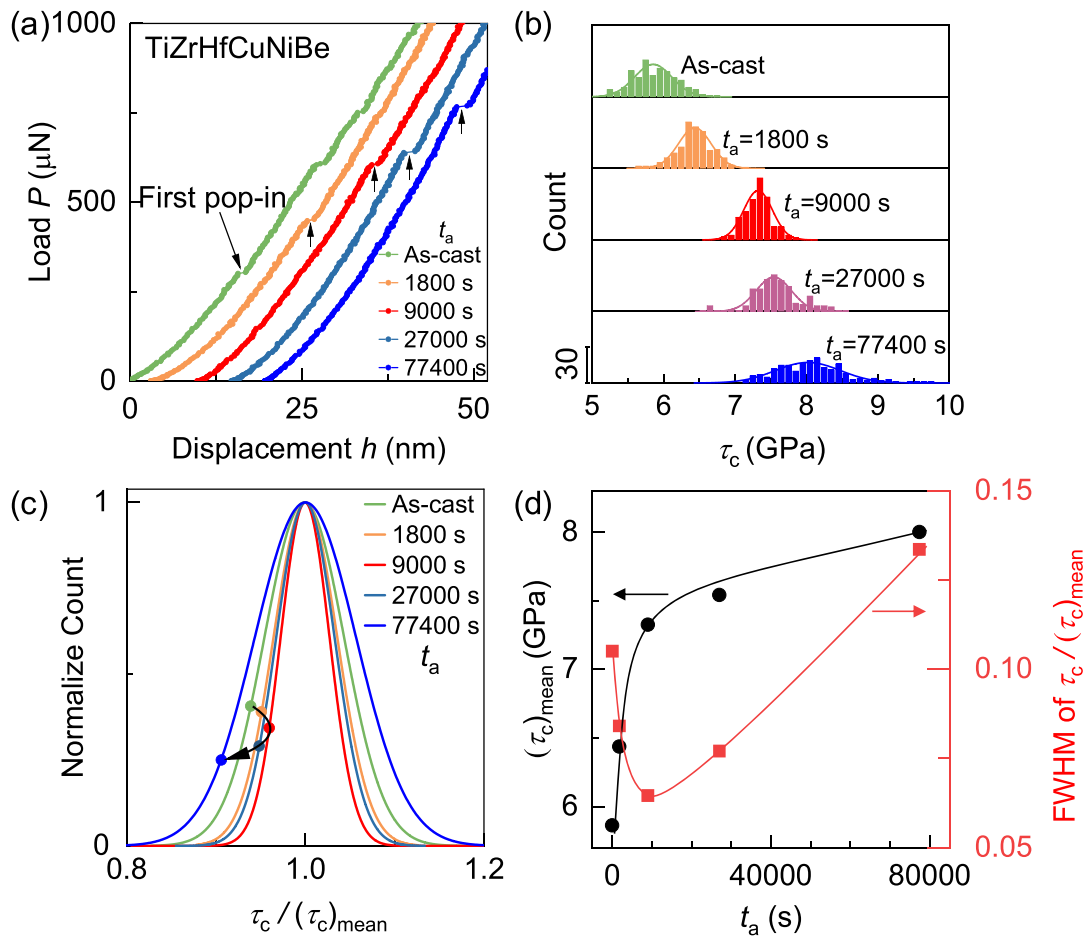


**Fig. 2.** Spatial heterogeneity. (a) Enlarged segments of room-temperature  $P$ - $h$  curves of TiZrHfCuNiBe samples after being annealed at 633 K for different annealing times  $t_a=0$ –77,400 s ( $t_a=9000$  s corresponds to the turning point of the  $\beta_{KWW}$ ) and the first pop-in events are marked by black arrows. (b) Aging effect on the statistical distribution of  $\tau_c$  for different  $t_a$ . (c) Gaussian fitting curves for normalized  $\tau_c/(\tau_c)_{\text{mean}}$ . (d) Change of mean critical shear stress  $(\tau_c)_{\text{mean}}$  (circle), and FWHM of the  $\tau_c/(\tau_c)_{\text{mean}}$  (square) with pre-annealing time  $t_a$ .

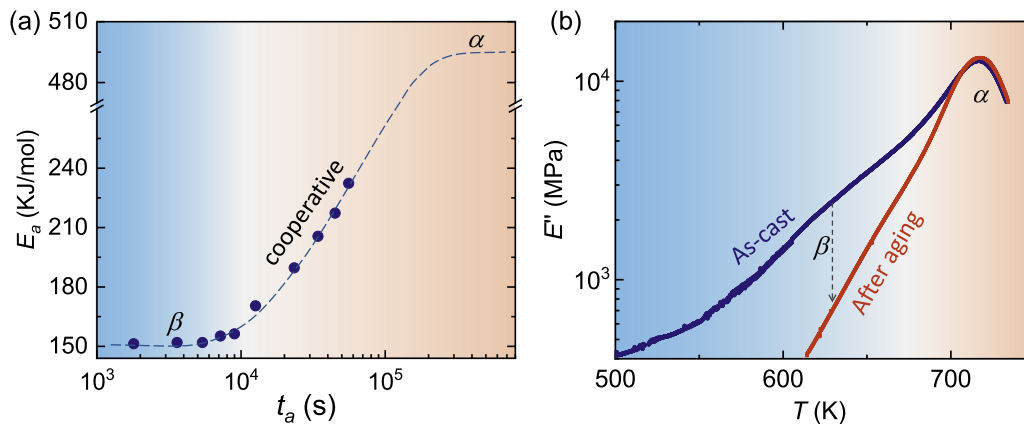


**Fig. 3.** Evolution of relaxation modes during aging. (a) Relaxation activation energy  $E_a$  versus the aging time  $t_a$ . (b) Loss modulus  $E''$  of the as-cast TiZrHfCuNiBe sample (blue) and the sample pre-aged at  $T_a=633$  K for  $t_a=77,400$  s (red). The data is measured with a frequency of 1 Hz at a heating rate of 3 K/min.

$E_\beta \approx 26(\pm 4)RT_g$  [58–60]. This suggests that the  $\beta$  relaxation dominates during the initial aging stage, which makes glasses more homogeneous with the increased  $\beta_{KWW}$  (see Fig. 1(c)). In the second stage, the activation energy ( $E_a$ ) undergoes a rapid increase towards the cooperative process, but is still much lower than the  $\alpha$  relaxation ( $E_\alpha=494.4$  kJ/mol, see Section 2 in Supplementary Information). This suggests that the atomic motions are more cooperative than the  $\beta$  relaxation, which is consistent with previous

works [39]. The results indicate that the aging driven by cooperative motion makes glasses more heterogeneous with the decreased  $\beta_{KWW}$  and broader  $\tau_c$  distribution. After isothermal annealing, the loss modulus curve  $E''$  in the dynamical mechanical spectrum confirms that the  $\beta$  relaxation peak has been depressed, as shown in Fig. 3(b).

The complex relaxations kinetics related to the heterogeneous structure interpreted that the looser atomic-packing soft domains

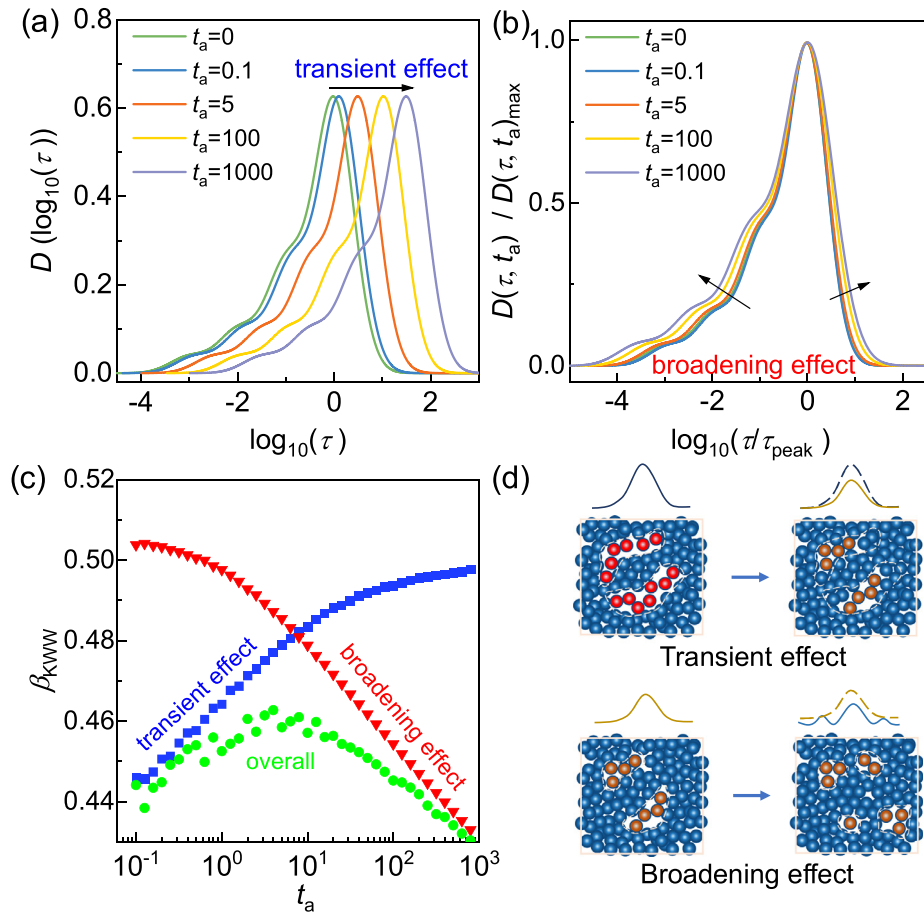


**Fig. 4.** Phenomenological description. Evolution of the relaxation time distribution considering (a) an invariant shape of  $D(\log(\tau))$  shifted by aging, and (b) normalized  $t_a$ -dependent shape  $D(\tau, t_a)$ , which corresponds to the normalized scaling of Fig. S10 with a reference aging time  $t_a=0$ ; (c) Evolution of  $\beta_{KWW}$  obtained considering: the transient effect generated by the shift of the invariant relaxation time distribution (blue squares), the broadening of the distribution as the function of aging time (red triangles), and both transient and broadening effects (green circles). (d) Schematic microscopic evolution for transient effect and broadening effect. The dashed loops mark the mobile atoms (red/dark red spheres), and the corresponding spatial fluctuations are illustrated roughly by overhead curves.

dispersed in the hard domains [5,8,29,38]. The  $\beta$  relaxation is closely related to the localized motion in isolated soft domains, while the ample motion sites percolating through the hard domains generate the cooperative  $\alpha$  relaxation [5,40]. Considering such a microstructural heterogeneity, a phenomenological model based on the  $\tau_c$  fluctuation is proposed to address the nonmonotonic behavior of  $\beta_{KWW}$ . We first consider a transient effect in which the size of the localized soft domains decreases, according to the increase of  $\tau_{KWW}$  and mean critical shear stress  $(\tau_c)_{\text{mean}}$  [5,38,46,61]. As shown in Fig. 4(a), a phenomenological model is proposed considering relaxation time distributions  $D(\tau)$  with the invariant shape that shifts to longer times upon annealing. The relaxation time follows the unified aging law  $\tau(t) = \tau_0 + At^\mu$  with  $\mu = 0.5$ . The corresponding evolution of stress decay is determined by  $\phi(t') = \int_0^\infty \varphi_\tau(t')D(\tau)d\tau$  with  $d\varphi_\tau = -\frac{\varphi_\tau(t')}{\tau(t')}dt'$  [5], where  $t' = t - t_a$  is the time of the stress relaxation test after isothermal annealing  $t_a$ . The detailed analysis can be found in Section 3 in Supplementary Information. The estimated  $\beta_{KWW}$  increases monotonically with  $t_a$ , as shown by the blue squares in Fig. 4(c), consistent with the initial aging of experimental results.

For the second stage, the broadened  $H$ -distribution and rapidly increased activation energy denote that more active sites in diverse cooperative motions have been triggered. This suggests the broadening of the distribution for relaxation modes. As shown in Fig. 4(b), we now consider a distribution  $D(\tau, t_a)$  of relaxation

modes broaden along with the increase of annealing time  $t_a$ . The relaxation curve is given by  $\phi(t') = \int_0^\infty e^{-t'/\tau}D(\tau, t_a)d\tau$  (see Fig. S10). The estimated  $\beta_{KWW}$  decreases monotonically along with the increase of annealing time, which is consistent with the deep aging stage in experimental results. Thus, as shown in Fig. 4(c), the combination of transient effect and broadening effect will cause the nonmonotonic changing behavior in  $t_a$ -dependent  $\beta_{KWW}$ .

Fig. 4(d) shows a schematic illustration of the microstructure evolution of metallic glass upon isothermal annealing. For the initial  $\beta$  relaxation stage with transient effect, the atoms that have low packing density exhibit string-like motions as suggested in Refs [62,63]. Giordano et al. [29] demonstrate that the low-density zones will become denser and density inhomogeneity is released upon this aging stage, while Ge et al. [16] observe that the atomic packing becomes more ordered with an increase in the height of the first diffraction peak. However, the work by Ge et al. [16] involves the release of external stress, which may be slightly different from the aging of as-cooled glass. The homogenization of glasses in the initial aging stage is accompanied by the annihilation of  $\beta$  relaxations which should be universal for different types of glasses, even though the structural origins of  $\beta$  relaxation for metallic glasses and polymer glasses are distinct, i.e.  $\beta$  relaxation in the polymer is related to the branched chains [64] but metallic glasses have no branched chains. This is attributed to the close relation between  $\beta$  relaxation and low-density regions [29,62,64,65].

For the second deep aging stage, the atomic motions become more cooperative with an increase in activation energy, which makes the microstructure of glasses heterogeneous. This is consistent with the observation of Ge et al. [16] that the glass gets into a state with more disordered regions with a decrease in the height of the first diffraction peak. Giordano et al. [29] think this process does not change the density.

Most metallic glasses show stretching exponents  $\beta_{KWW}$  near 0.5 associated with the sub- $T_g$  aging process [40,66], a similar value is also observed for the MGs of this work. The interesting point here is that during the path towards equilibrium, the exponent  $\beta_{KWW}$  decreases, implying an increase of dynamical heterogeneity. This indicates that aging not only shifts the average relaxation time, but also alters the distribution of relaxation modes, and aging cannot be understood as a mere reduction of soft domains, which would produce a homogenization of the glass structure. Considering that the relaxation curve is given by  $\phi(t') = \int_0^\infty e^{-t'/\tau} D(\tau, t_a) d\tau$  with a  $t_a$ -dependent distribution  $D(\tau, t_a)$  of relaxation modes, it is found that the aging broadens the distribution  $D(\tau, t_a)$  and reduces  $\beta_{KWW}(t_a)$ . Such increasing in dynamical heterogeneity with aging coincides with an increase in structural heterogeneity, identified by the broader distribution of critical shear stress for local plasticity. This is unexpected and contrary to the conventional idea that annealing toward equilibrium usually homogenizes the glass structure.

## 5. Conclusion

In summary, we studied the aging effect on the relaxation kinetics and structural heterogeneity of glasses by stress relaxation and nanomechanical tests, respectively. The relaxation kinetics is analyzed by using the stretched exponential equation. An unexpected two-stage nonmonotonic evolution of the stretching exponent  $\beta_{KWW}$  is observed, that is,  $\beta_{KWW}$  first increases and then decreases. The as-quenched glass that has pronounced slow- $\beta$  relaxation is heterogeneous. Upon isothermal annealing, the slow- $\beta$  relaxation is triggered and progressively annihilated, and the glass becomes homogeneous. However, when the annealing time is long enough and the cooperative motion is triggered, the glass becomes more heterogeneous again, confirmed by the broader distribution of critical shear stress for local plasticity. These observations clarify the arguments in traditional views of the aging effects on glasses. The results obtained for various glassy systems suggest that such a nonmonotonic effect upon annealing is probably universal in glasses. Our findings shed new light on comprehensively understanding the annealing effect on glasses and might be useful in developing advanced glassy materials.

## Declaration of Competing Interest

The authors declare that they have no known competing financial interests or personal relationships that could have appeared to influence the work reported in this paper.

## Acknowledgements

This work was financially supported by the National Natural Science Foundation of China (Nos. 52201193, 51922102, 92163108 and 52001319), the National Key R&D Program of China (No. 2018YFA0703600), the Ningbo Natural Science Foundation of Ningbo City (No. 2022J310), the "Pioneer and Leading Goose" R&D Program of Zhejiang (No. 2022C01023), 'Proyecto PID2020-112975GB-I00 de investigación financiado por MCIN/AEI/10.13039/501100011033', Generalitat de Catalunya AGAUR grant 2017-SGR-42.

## Supplementary materials

Supplementary material associated with this article can be found, in the online version, at doi:10.1016/j.jmst.2023.07.071.

## References

- [1] L. Berthier, *Physics* (College Park Md) 4 (2011) 42.
- [2] H.E. Castillo, C. Chamon, L.F. Cugliandolo, M.P. Kennett, *Phys. Rev. Lett.* 88 (2002) 237201.
- [3] M.D. Ediger, *Annu. Rev. Phys. Chem.* 51 (2000) 99.
- [4] Y. Liu, D. Wang, K. Nakajima, W. Zhang, A. Hirata, T. Nishi, A. Inoue, M. Chen, *Phys. Rev. Lett.* 106 (2011) 125504.
- [5] W.H. Wang, *Prog. Mater. Sci.* 106 (2019) 100561.
- [6] H. Ke, J. Zeng, C. Liu, Y. Yang, *J. Mater. Sci. Technol.* 30 (2014) 560–565.
- [7] J.P. Wu, Y. Lin, F.H. Duan, Q. Chen, H.T. Wang, N. Li, J.L. Wen, J. Pan, L. Liu, *J. Mater. Sci. Technol.* 63 (2023) 140–149.
- [8] Z. Wang, B. Sun, H. Bai, W. Wang, *Nat. Commun.* 5 (2014) 5823.
- [9] C. Chang, H. Zhang, R. Zhao, F. Li, P. Luo, M. Li, H. Bai, *Nat. Mater.* 21 (2022) 1240–1245.
- [10] Y. Cheng, E. Ma, *Prog. Mater. Sci.* 56 (2011) 379–473.
- [11] J. Ye, J. Lu, C. Liu, Q. Wang, Y. Yang, *Nat. Mater.* 9 (2010) 619–623.
- [12] S. Ketov, Y. Sun, S. Nachum, Z. Lu, A. Checchi, A. Beraldin, H. Bai, W. Wang, D. Louzguine-Luzgin, M. Carpenter, *Nature* 524 (2015) 200–203.
- [13] H. Yu, X. Shen, Z. Wang, L. Gu, W. Wang, H. Bai, *Phys. Rev. Lett.* 108 (2012) 015504.
- [14] R. Qu, C.A. Volkert, Z. Zhang, F. Liu, *J. Mater. Sci. Technol.* 149 (2023) 247–254.
- [15] S. Liu, W. Dong, Z. Ren, J. Ge, S. Fu, Z. Wu, J. Wu, Y. Lou, W. Zhang, H. Chen, W. Yin, Y. Ren, J. Neuefeind, Z. You, Y. Liu, X.L. Wang, S. Lan, *J. Mater. Sci. Technol.* 159 (2023) 10–20.
- [16] J. Ge, P. Luo, Z. Wu, W. Zhang, S. Liu, S. Lan, J.D. Almer, Y. Ren, X.L. Wang, *W. Wang, Mater. Res. Lett.* 11 (2023) 547–555.
- [17] S. Ouyang, L. Song, Y. Liu, J. Huo, J. Wang, W. Xu, J. Li, C. Wang, X. Wang, R. Li, *Phys. Rev. Mater.* 2 (2018) 063601.
- [18] C. Zhao, A. Wang, A. He, C. Chang, C.T. Liu, *Sci. China Mater.* 64 (2021) 1813–1819.
- [19] H. Yin, J.Q. Wang, Y. Huang, H. Shen, S. Guo, H. Fan, J. Huo, J. Sun, *J. Mater. Sci. Technol.* 149 (2023) 167–176.
- [20] R. Richert, *Phys. Rev. Lett.* 104 (2010) 085702.
- [21] W. Kob, J.L. Barrat, *Phys. Rev. Lett.* 78 (1997) 4581.
- [22] Y. Zhao, B. Shang, B. Zhang, X. Tong, H. Ke, H. Bai, W.H. Wang, *Sci. Adv.* 8 (2022) 3623.
- [23] Y. Meng, S. Zhang, W. Zhou, J. Yao, S. Liu, S. Lan, Y. Li, *Acta Mater.* 241 (2022) 118376.
- [24] C.A. Angell, *Science* 267 (1995) 1924–1935.
- [25] P. Luo, M. Li, H. Jiang, P. Wen, H. Bai, W. Wang, *J. Appl. Phys.* 121 (2017) 135104.
- [26] P. Tsai, K. Kranjc, K.M. Flores, *Acta Mater.* 139 (2017) 11–20.
- [27] F. Zhu, S. Song, K.M. Reddy, A. Hirata, M. Chen, *Nat. Commun.* 9 (2018) 3965.
- [28] Y. Lü, C. Guo, H. Huang, J. Gao, H. Qin, W. Wang, *Acta Mater.* 211 (2021) 116873.
- [29] V. Giordano, B. Ruta, *Nat. Commun.* 7 (2016) 10344.
- [30] P. Luo, P. Wen, H. Bai, B. Ruta, W. Wang, *Phys. Rev. Lett.* 118 (2017) 225901.
- [31] Z. Evenson, B. Ruta, S. Hechler, M. Stolpe, E. Pineda, I. Gallino, R. Busch, *Phys. Rev. Lett.* 115 (2015) 175701.
- [32] L. Song, W. Xu, J. Huo, J.Q. Wang, X. Wang, R. Li, *Intermetallics* 93 (2018) 101–105.
- [33] E. Pineda, P. Bruna, B. Ruta, M. Gonzalez-Silveira, D. Crespo, *Acta Mater.* 61 (2013) 3002–3011.
- [34] J. Hachenberg, D. Bedorf, K. Samwer, R. Richert, A. Kahl, M.D. Demetriou, W.L. Johnson, *Appl. Phys. Lett.* 92 (2008) 131911.
- [35] M. Mao, Z. Altounian, R. Brüning, *Phys. Rev. B* 51 (1995) 2798.
- [36] D. Soriano, H. Zhou, S. Hilke, E. Pineda, B. Ruta, G. Wilde, *J. Phys.: Condens. Mater.* 33 (2021) 164004.
- [37] N. Amini, F. Yang, E. Pineda, B. Ruta, M. Sprung, A. Meyer, *Phys. Rev. Mater.* 5 (2021) 055601.
- [38] B. Ruta, Y. Chushkin, G. Monaco, L. Cipolletti, E. Pineda, P. Bruna, V. Giordano, M. Gonzalez-Silveira, *Phys. Rev. Lett.* 109 (2012) 165701.
- [39] L. Song, M. Gao, W. Xu, J. Huo, J. Wang, R. Li, W. Wang, J. Perepezko, *Acta Mater.* 185 (2020) 38–44.
- [40] J. Qiao, Q. Wang, J. Pelletier, H. Kato, R. Casalini, D. Crespo, E. Pineda, Y. Yao, Y. Yang, *Prog. Mater. Sci.* 104 (2019) 250–329.
- [41] Y. Duan, L. Zhang, J. Qiao, Y.J. Wang, Y. Yang, T. Wada, H. Kato, J. Pelletier, E. Pineda, D. Crespo, *Phys. Rev. Lett.* 129 (2022) 175501.
- [42] F. Zhu, H. Nguyen, S. Song, D.P. Aji, A. Hirata, H. Wang, K. Nakajima, M. Chen, *Nat. Commun.* 7 (2016) 11516.
- [43] Y. Yang, J. Zeng, A. Volland, J. Blandin, S. Gravier, C.T. Liu, *Acta Mater.* 60 (2012) 5260–5272.
- [44] H. Zhou, V. Khonik, G. Wilde, *J. Mater. Sci. Technol.* 103 (2022) 144–151.
- [45] K.L. Johnson, K.L. Johnson, *Contact Mechanics*, Cambridge University Press, 1987.
- [46] Y. Wu, D. Cao, Y. Yao, G. Zhang, J. Wang, L. Liu, F. Li, H. Fan, X. Liu, H. Wang, *Nat. Commun.* 12 (2021) 6582.
- [47] L.M. Wang, R. Liu, W.H. Wang, *J. Chem. Phys.* 128 (2008) 164503.
- [48] R. Richert, *J. Phys.: Condens. Mater.* 14 (2002) R703.
- [49] S. Capaccioli, M. Paluch, D. Prevosto, L.M. Wang, K. Ngai, *J. Phys. Chem. Lett.* 3 (2012) 735–743.

- [50] L.C.E. Struik, *Physical Aging in Amorphous Polymers and Other Materials*, Elsevier, 1977.
- [51] L. Cipolletti, S. Manley, R. Ball, D. Weitz, *Phys. Rev. Lett.* 84 (2000) 2275.
- [52] L. Ramos, L. Cipolletti, *Phys. Rev. Lett.* 87 (2001) 245503.
- [53] C. Liu, R. Maaß, *Adv. Funct. Mater.* 28 (2018) 1800388.
- [54] L. Huo, J. Zeng, W. Wang, C.T. Liu, Y. Yang, *Acta Mater.* 61 (2013) 4329–4338.
- [55] I.C. Choi, Y. Zhao, B.G. Yoo, Y.J. Kim, J.Y. Suh, U. Ramamurty, J.I. Jang, *Scr. Mater.* 66 (2012) 923–926.
- [56] H. Fan, X. Liu, H. Wang, Y. Wu, Z. Lu, *Intermetallics* 90 (2017) 159–163.
- [57] P. Ross, S. Küchemann, P.M. Derlet, H. Yu, W. Arnold, P. Liaw, K. Samwer, R. Maaß, *Acta Mater.* 138 (2017) 111–118.
- [58] H.B. Yu, W.H. Wang, H.Y. Bai, K. Samwer, *Natl. Sci. Rev.* 1 (2014) 429–461.
- [59] L. Hu, Y. Yue, *J. Phys. Chem. C* 113 (2009) 15001–15006.
- [60] K. Ngai, S. Capaccioli, *Phys. Rev. E* 69 (2004) 031501.
- [61] R. Maaß, P. Derlet, *Acta Mater.* 143 (2018) 338–363.
- [62] H.B. Yu, R. Richert, K. Samwer, *Sci. Adv.* 3 (2017) 1701577.
- [63] Y.C. Hu, H. Tanaka, *Nat. Phys.* 18 (2022) 669–677.
- [64] N.G. Perez-De-Eulate, D. Cangialosi, *Macromolecules* 51 (2018) 3299–3307.
- [65] G. Johari, *J. Non-Cryst. Solids* 307 (2002) 317–325.
- [66] R. Casalini, C. Roland, *Phys. Rev. Lett.* 102 (2009) 035701.